Sectorised Horn Antenna Array Using an RF MEMS Rotary Switch

S. Pranonsatit [1], A. S. Holmes [2] and S. Lucyszyn [2*]
[1] *Department of Electrical Engineering, Kasetsart University, Bangkok, Thailand*
[2] *Optical and Semiconductor Devices Group, Department of Electrical and Electronic Engineering Imperial College London, Exhibition Road, London, SW7 2AZ, United Kingdom*
[*] s.lucyszyn@imperial.ac.uk

***Abstract* — A sectorised horn antenna array, comprising eight Vivaldi antennas and a single-pole multiple-throw RF MEMS rotary switch, has been demonstrated for the first time. Details of the design and fabrication are presented, together with preliminary measurements for a proof-of-concept prototype which confirm the principle of operation. It is believed that with further work a much higher performance can be achieved.**

***Index Terms* — Sectorised antenna array, horn antenna, RF MEMS, rotary switch.**

I. INTRODUCTION

Radio frequency microelectromechanical systems (RF MEMS) technology can offer enhanced performance compared to solid-state devices (e.g. switches and varactor diodes), in terms of factors that can include performance figure-of-merit and RF power nonlinearity [1]. There are a number of notable examples of antennas that employ RF MEMS devices. These can be divided into two distinct categories: *generic RF MEMS antennas* and *RF MEMS antenna circuits*. The former have radiating elements that physically move under some form of actuation mechanism, while the latter have fixed position radiating elements that employ RF MEMS switches or variable capacitors to alter their electrical behaviour [1].

The first generic RF MEMS antenna was reported just over a decade ago by Chiao *et al.* [2, 3]. Here, the arms of a Vee-antenna were independently controlled using linear scratch drive actuators. As a result, the azimuthal pointing direction and directivity of the main beam could be controlled independently. More recently, a V-band single-platform beam steering transmitter [4] was demonstrated by employing an antenna having two degrees of rotational freedom around torsion bar hinges, with an external magnetic force being used for actuation [5, 6].

There are many examples of RF MEMS antenna circuits. Multi-band operation has been demonstrated using RF MEMS switches within fractal antennas [7]. Strategically placed switches can control the currents in the branches of the antenna, modifying the resonance behaviour of the entire structure and its radiation pattern. For example, using a Sierpinski Gasket design, a reconfigurable antenna was demonstrated based on this principle [7]. More recently, much simpler dual-frequency reconfigurable slot dipole arrays for X- and Ka-band [8] and Ka- and V-band [9] were reported in which RF MEMS switches were placed across the slots. Similarly, a single-arm spiral antenna with RF MEMS switches located along the line was reported for X-band operation [10].

Thermo-compression wafer bonding techniques have also been employed to realize a 3-layer tuneable coplanar patch antenna (TCPA) with RF MEMS varactor [11-12]. Also, a 35 GHz coupled patch antenna array has been demonstrated within a multi-layer LTCC module [13]. Here, flip-chip mounted RF MEMS phase shifter chips were integrated between the feed network and a serially fed patch antenna array, to implement 1D beam steering. Moreover, wafer bonding by cross linking SU8 was realized in a MEMS programmable lens-array (MPLA) antenna [14].

In addition, at X-band, a 4 x 8 patch antenna array was realized on a Teflon substrate, with a hybrid integration of silicon RF MEMS phase shifters for performing beam steering [15]. The same team went on to demonstrate a data link at Ka-band, with the RF MEMS phase shifter chips placed within 3-layer LTCC cavities [16].

In this paper we report on the design, fabrication and measured performance of a novel RF MEMS antenna circuit in the form of a sectorised horn antenna. The device consists of eight Vivaldi antennas fabricated on a flexible organic substrate, with a central single-pole-eight-throw (SP8T) RF MEMS rotary switch for antenna selection.

The Vivaldi antenna is an end-fired tapered slot antenna (TSA) [17]. The slot is smoothly tapered from narrow to wide to give it an ultra-wideband (UWB) performance [18]. Vivaldi antennas generally exhibit high gain and linear polarization. Compared to other UWB solutions, Vivaldi antennas benefit from compactness, simplicity and an adjustable beamwidth. Since 1974 [19], various Vivaldi antenna designs have been reported [20-28]. Moreover, the issue of mutual coupling effects on bandwidth in Vivaldi antenna arrays has also been investigated [29-30]. While it is believed that mutual coupling can improve bandwidth, when compared to an isolated Vivaldi element [31] it has been shown that mutual coupling has a negative effect on bandwidth, although this can be improved by including chokes that attenuate currents between elements. Vivaldi antennas have already been used with RF MEMS. Examples include a 10 GHz analog slotline true time delay (TTD) phase shifter [32], an UWB near-field imaging system [33] and a

16-element phased sub-array with Ka band phase shifters [34].

In the past single-pole multiple-throw RF MEMS switches have been realized mainly by integrating a number of single-pole single-throw (SPST) switches. However, as the number of bits increases, this solution can be unwieldy and result in yield and reliability issues. For example, a discrete single-pole eight-throw (SP8T) switch may require about 15 times the real estate of an SPST switch and 8 separate moving parts. In contrast, and as a new application demonstrator, the switch used in the present work is relatively compact and has only one moving part [35]. This switch has already been demonstrated within a 2-bit digital TTD phase shifter application [36].

II. Antenna Designs and Fabrication

Figure 1 shows the overall layout of the sectored antenna array. The SP8T RF MEMS switch was fabricated on a 500 μm-thick quartz substrate with gold and nickel metallization layers, while the Vivaldi antenna array was made on a 250 μm-thick Taconic RF-35 laminate with gold-plated copper cladding.

The RF MEMS rotary switch is based on the axial-gap wobble motor principle. In this kind of device, the rotor is tilted, with its centre on a raised bearing and one side pulled down by electrostatic attraction to underlying drive electrodes so that a point on its periphery rests on the stator [35]. By exciting the drive electrodes in sequence, the rotor can be made to perform a precessional motion whereby the physical contact between rotor and stator rotates continuously around the periphery of the device. To allow RF switching, the stator has one input CPW transmission line which extends underneath the rotor and connects to the central bearing, and eight output CPW lines which terminate at points around the periphery. The RF signal is continuously fed to the rotor via the inherent Ohmic contact between the touching surfaces of rotor and bearing, and the signal may be routed to any desired output port simply by moving the rotor until it also forms an Ohmic contact with the corresponding output CPW line.

Gold bond wires were used to connect the CPW lines on the switch to microstrip lines on the Taconic RF-35 laminate, as illustrated in Fig. 1(a). The RF signals from the microstrip lines are coupled to the associated slotlines beneath, and then radiated via the tapered slots of the Vivaldi antennas, as shown in Fig. 1(b). The individual Vivaldi antennas were housed in their own pyramidal horns in order to greatly increase directivity. Separation slots were introduced into the RF-35 laminate to accommodate the horns, as illustrated in Fig. 1(b).

It can be seen in Fig. 1(a) that the main RF input signal is fed to the SP8T switch via an SMA connector underneath the Taconic RF-35 laminate and bond wires above. The dc bias pin connectors were connected in a similar way as the SMA connector. Ground connections between the antenna and the CPW-to-microstrip transition were made using plated-through vias.

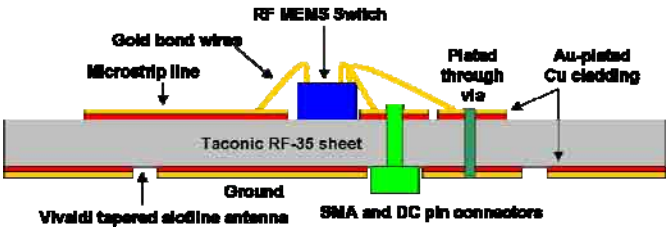

(a)

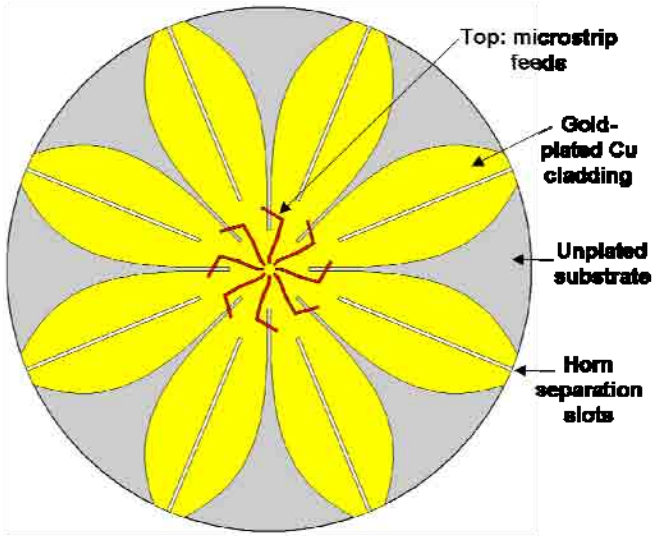

(b)

Fig. 1. Schematic views of complete antenna array (not to scale) showing: (a) switch/antenna integration; and (b) top (red) and bottom (yellow) metallization of Taconic RF-35 laminate.

In designing the antenna, the value for the effective thickness of the substrate, normalized to the free space wavelength at centre frequency, should be within the optimal range given by equation (1) [24]:

$$0.005 \le \frac{\left(\sqrt{\varepsilon_r} - 1\right)t}{\lambda_0} \le 0.03 \qquad (1)$$

where ε_r and t are the dielectric constant and physical thickness of the radiating substrate, respectively, and λ_0 is the free-space wavelength at the centre frequency of operation. The beam width will be too wide on thinner substrates, whereas the main beam will break up for thicker substrates.

The Taconic RF-35 laminate substrate has a circular shape, with a 30 cm diameter, 250 μm physical thickness, and an 18 μm-thick electrodeposited Cu cladding on each side (plated with 0.5 μm-thick gold). The dielectric constant and $tan\delta$ are 3.5 and 18 x 10^{-4}, respectively. Therefore, at a center frequency of 10 GHz, the normalized effective thickness for this laminate is 0.0073, which is within the optimum range. The effective radiating length of the antenna is $5\lambda_0$, i.e. within the recommended range of 2 to 12 λ_0 [37].

The assembled sectorised horn antenna array is shown in Fig. 2. Fig. 2(a) show eight individual 20 dBi gain pyramidal horns, made from double-clad FR-4 substrate material, attached at the edges of the horn separation slots in the Taconic RF-35 laminate substrate. Fig. 2(b) shows a close-up view of the centre of the antenna array, where the rotary switch and microstrip lines are located. Microwave absorber is included to minimize coupling between adjacent antennas. The side view at the antenna array is shown in Fig. 2(c).

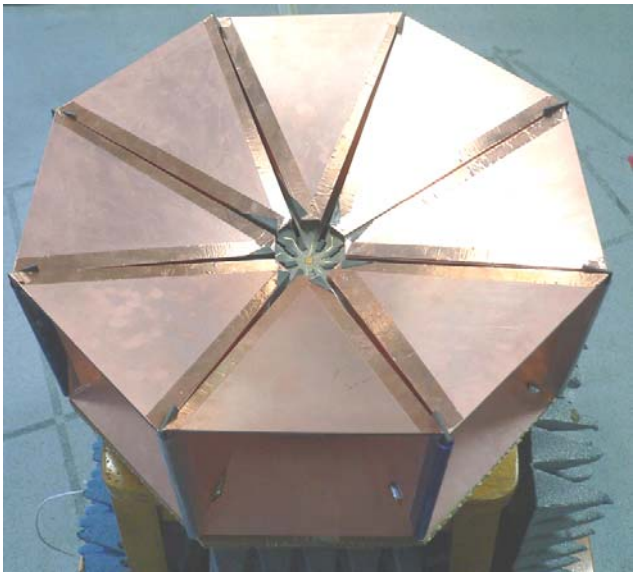

(a)

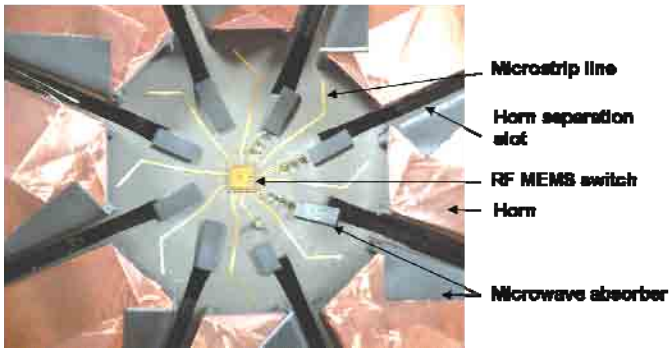

(b)

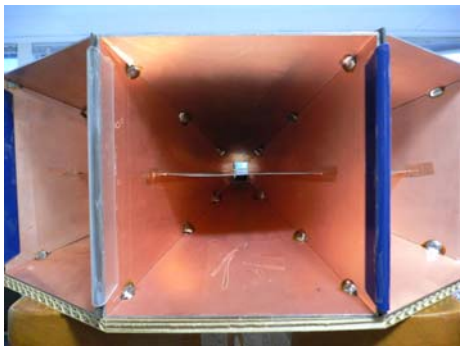

(c)

Fig. 2. The assembled RF MEMS sectorised antenna array: (a) top view; (b) close-up view at the centre and (c) side view.

The diameter of the antenna array was chosen to match the size of the RF-35 laminate sheet, which was 30 cm × 30 cm. Each antenna was assigned a 45º slice of the circle. The dimensions of the microstrip line and slotline feeds were calculated using Agilent's *LineCalc* software. The curvature of the tapered slotline follows an exponential profile [25, 38], defined by the following:

$$y = 0.5e^{0.04x} \qquad (2)$$

where x is the distance along the slotline and y is the width.

This curvature results in an opening flare (in the y-axis) of 36º. This optimized angle is constrained by the width of the antenna's aperture and the degree of curvature. The latter determines the performance of the antenna. Specifically, when the degree of curvature is increased, the beamwidth is increased but the bandwidth and return loss are reduced [38].

III. Measurements

The initial design reported here did not include proper impedance matching for the SP8T RF MEMS rotary switch. This, together the relatively long (1 to 2 mm length) bond wire interconnects, resulted in far from optimal performance. Measurements of the overall input return loss for the complete antenna array, between 6 and 14 GHz and when the switch is making contact in all eight positions, are shown in Fig. 3. It can be seen that best performance is achieved at approximately 7 and 13 GHz.

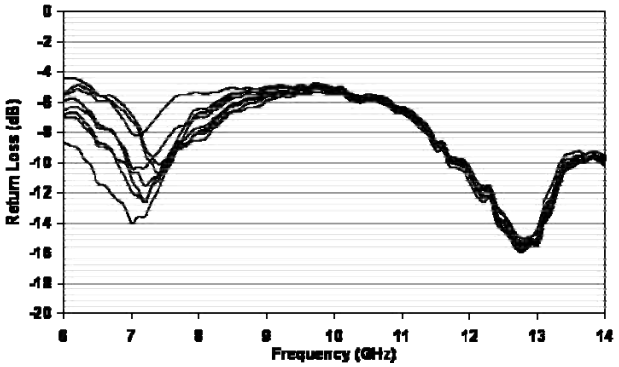

Fig. 3. Measured antenna array return loss at all 8 switch positions.

Due to a lack of suitable resources, the E-plane radiation pattern could not be measured within an anechoic chamber. Instead the measurement setup was rather crude and located inside a large room. While this measurement environment is far from ideal (due to problems associated with reflections from walls, windows, ceiling, floor and metal objects) it does give some preliminary qualitative results for the antenna radiation patterns in the E-plane.

The antenna was fed by a square-wave-modulated 10 GHz signal source, protected by an output isolator. A measurement setup to detect the received power (consisting of a reference pyramidal horn, a Schottky diode square law detector and a

high gain IF amplifier) was then rotated around the sectorised horn antenna array in steps of either 1º or 2º.

With the SP8T RF MEMS rotary switch set to output position #3, the E-plane radiation pattern for the assembled sectorised horn antenna array was measured within the non-ideal environment. The preliminary results are shown in Fig. 4(a). In addition, Fig. 4(b) shows the results for the individual main beams when the switch is set to all eight positions.

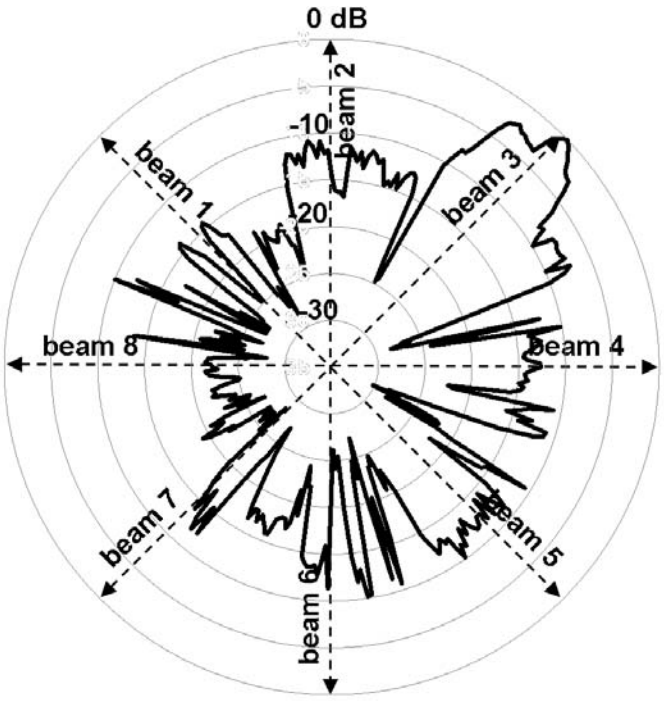

(a)

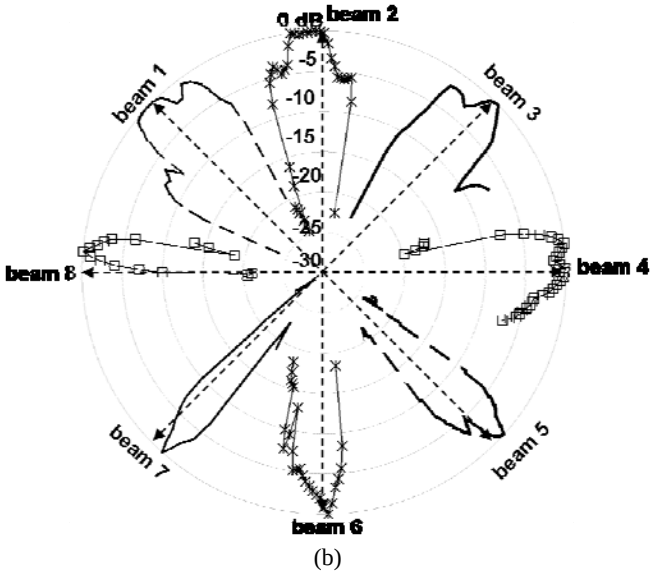

(b)

Fig. 4. Measured radiation patterns for the sectorised horn antenna array (normalized to beam centres): (a) at switch/beam position #3 and (b) superimposed main beams for all eight switch positions.

V. Conclusions

A sectorised horn antenna array, employing a single-pole multiple-throw RF MEMS rotary switch, has been demonstrated for the first time. Even though the design of this proof-of-concept demonstrator is not optimal, and the test environment was far from ideal, preliminary measurements confirm the principle of operation for this novel antenna array. It is believe that with further work (e.g. optimization of the switch, individual radiating antenna elements and array assembly) a higher performance can be achieved.

Acknowledgements

The authors would like to thank the Thailand Research Fund (TRF) for their financial support of this research project, under grant number MRG5180264, and the Faculty of Engineering, Kasetsart University, under grant 50/16/EE. We are also grateful for Dr. Denchai Worasawate, Kasetsart University, for his valuable comments.

In addition, this work was supported by the UK Engineering and Physical Sciences Research Council (EPSRC), under Platform Grant EP/E063500/1. The RF-35 substrates used in this project were kindly donated by Taconic Advanced Dielectric Division.

References

[1] S. Lucyszyn (Editor), "Advanced RF MEMS", Cambridge University Press, Cambridge, Sep. 2010

[2] J.-C. Chiao, Y. Fu, I. M. Chio, M. DeLisio and L.-Y. Lin, "MEMS reconfigurable Vee antenna", *IEEE MTT-S International Microwave Symposium Digest*, Anaheim, CA, pp. 1515-1518, 1999

[3] J.-C. Chiao, Y. Fu, D. Choudhury and L.-Y. Lin, "MEMS millimeterwave components", *IEEE MTT-S International Microwave Symposium Digest*, Anaheim, CA, pp. 463-466, 1999

[4] S. Lee, J.-M. Kim, J.-M. Kim, Y.-K, Kim, C. Cheon, and Y. Kwon, "V-band single-platform beam steering transmitters using micromachining technology", *IEEE MTT-S International Microwave Symposium Digest*, San Francisco, CA, pp.148-15, 2006

[5] C.-W. Baek, S. Song, C. Cheon, Y.-K. Kim and Y. Kwon, "2-D mechanical beam steering antenna fabricated using MEMS technology" *IEEE MTT-S International Microwave Symposium Digest*, San Francisco, CA, pp.211-214, 2001

[6] C.-W. Baek, S. Song, J.-H. Park, S. Lee, J.-M. Kim, W. Choi, C. Cheon, Y.-K. Kim and Y. Kwon, "A V-band micromachined 2-D beam-steering antenna driven by magnetic force with polymer-based hinges", *IEEE Transactions on Microwave Theory and Techniques*, vol. 51, no. 1, pp. 325-331, Jan. 2003

[7] C. G. Christodoulou, "RF-MEMS and its applications to microwave systems, antennas and wireless communications", *Proceedings of the SBMO/IEEE MTT-S International Microwave and Optoelectronics Conference*, Foz do Iguaçu, Brazil, pp. 525- 531, 2003

[8] K. Topalli, O. A. Civi, S. Demir, S. Koc and T. Akin, "Dual-frequency reconfigurable slot dipole array with a CPW-based feed network using RF MEMS technology for X- and Ka-band applications", *IEEE Antennas and Propagation Society International Symposium*, Honolulu, HI, pp. 825-828, 2007

[9] G. Liu, C. L. Law, M. J. Rajanik and H. Yang, "A switchable MEMS antenna for 38/60 GHz millimeter wave communications", *International Conference on Microwave and Millimeter Wave Technology Proceedings*, Beijing, China, pp. 86- 89, 2004

[10] C. W. Jung, M.-J. Lee, G. P. Li and F. De Flaviis, "Reconfigurable scan-beam single-arm spiral antenna integrated with RF-MEMS switches", *IEEE Transactions on Antennas and Propagation*, vol. 54, no. 2, pp. 455- 463, Feb. 2006

[11] M. Maddela, R. Ramadoss and R. Lempkowski, "PCB MEMS-Based tunable coplanar patch antenna", *IEEE International Symposium on Industrial Electronics*, Vigo, Spain, pp. 3255-3260, 2007

[12] A. Sundaram, M. Maddela, R. Ramadoss and L. M. Feldner, "MEMS-based electronically steerable antenna array fabricated using PCB technology", *Journal of Microelectromechanical Systems*, vol. 17, no. 2, pp. 356-362, Apr. 2008

[13] W. Gautier, B. Schoenlinner, V. Ziegler, U. Prechtel and W. Menzel, "LTCC patch array for RF-MEMS based phased array antenna at 35GHz" *38th European Microwave Conference*, Amsterdam, pp. 151-154, 2008

[14] C.-C. Cheng, B. Lakshminarayanan and A. Abbaspour-Tamijani, "A programmable lens-array antenna with monolithically integrated MEMS switches", *IEEE Transactions on Microwave Theory and Techniques*, vol. 57, no. 8, pp. 1874-1884, Aug. 2009

[15] W. Gautier, A. Stehle, C. Siegel, B. Schoenlinner, V. Ziegler, U. Prechtel and W. Menzel, "Hybrid integrated RF-MEMS phased array antenna at 10GHz" *38th European Microwave Conference*, Amsterdam, pp. 139-142, 2008

[16] W. Gautier, V. Ziegler, A. Stehle, B. Schoenlinner, U. Prechtel and W. Menzel, "RF-MEMS phased array antenna on low-loss LTCC substrate for ka-band data link", *European Microwave Conference*, Rome, pp. 914-917, 2009

[17] C. Zhang, M. Kuhn, M. Mahfouz and A. E. Fathy, "Planar antipodal Vivaldi antenna array configuration for low cross-polarization and reduced mutual coupling performance", *IEEE Antennas and Propagation Society International Symposium*, Honolulu, HI, pp. 725-728, 2007

[18] L. Ying and C. Ai-Xin, "Design and application of Vivaldi antenna array", *International Symposium on Antennas, Propagation and EM Theory*, Kunming, China, pp. 267-270, 2008

[19] L. R. Lewis, M. Fassett and J. Hunt, "A broadband stripline array element", *Antennas and Propagation Society International Symposium*, pp. 335- 337, 1974

[20] P. J. Gibson, "The Vivaldi aerial", *9th European Microwave Conference*, pp. 101-105, 1979

[21] A. Z. Hood, T. Karacolak and E. Topsakal, "A small antipodal Vivaldi antenna for ultrawide-band applications", *IEEE Antennas and Wireless Propagation Letters*, vol.7, pp. 656-660, Mar. 2008.

[22] D. Schaubert, E. Kollberg, T. Korzeniowski, T. Thungren, J. Johansson and K. Yngvesson, "Endfire tapered slot antennas on dielectric substrates", *IEEE Transactions on Antennas and Propagation*, vol. 33, no. 12, pp. 1392- 1400, Dec. 1985

[23] R. Janaswamy and D. Schaubert, "Analysis of the tapered slot antenna", *IEEE Transactions on Antennas and Propagation*, vol. 35, no. 9, pp. 1058-1065, Sep. 1987

[24] K. S. Yngvesson, T. L. Korzeniowski, Y.–S. Kim, E. L. Kollberg and J. F. Johansson, "The tapered slot antenna – a new integrated element for millimeter-wave applications", *IEEE Transactions on Microwave Theory and Techniques*, vol. 37, no. 2, pp. 365-374, Feb. 1989

[25] J. Shin and D. H. Schaubert, "A parameter study of stripline-fed Vivaldi notch-antenna arrays", *IEEE Transactions on Antennas and Propagation*, vol. 47, no. 5, pp. 879-886, May 1999

[26] T. G. Lim, H. N. Ang, I. D. Robertson, and B. L. Weiss, "Tapered slot antenna using photonic bandgap structure to reduce substrate effects", *Electronics Letters*, vol. 41, no. 7, pp. 393-394, Mar. 2005

[27] P. Li, J. Liang and X. Chen, "UWB tapered-slot-fed antenna", *The Institution of Engineering and Technology Seminar on Ultra Wideband Systems, Technologies and Applications*, London, pp. 235-238, 2006

[28] P. Cerny, J. Nevrly and M. Mazanek, "Optimization of tapered slot Vivaldi antenna for UWB application", *19th International Conference on Applied Electromagnetics and Communications*, Dubrovnik, pp. 1-4, 2007

[29] A. O. Boryssenko, D. H. Schaubert and C. Craeye, "A wave-based model for mutual coupling and truncation in finite tapered-slot phased arrays", *IEEE Antennas and Propagation Society International Symposium*, Columbus, OH, pp. 11-14, 2003

[30] M. Wang, W. Wu and C. Miao, "Mutual coupling effect on bandwidth of Vivaldi arrays", *IEEE Antennas and Propagation Society International Symposium*, Charleston, SC, pp.1-4, 2009

[31] A. O. Boryssenko and D. H. Schaubert, "Physical aspects of mutual coupling in finite broadband tapered slot (Vivaldi) arrays", *International Conference on Antenna Theory and Techniques*, Kyiv, Ukraine, pp. 74-79, 2005

[32] K. Van Caekenberghe and T. Vaha-Heikkila, "An analog RF MEMS slotline true-time-delay phase shifter", *IEEE Transactions on Microwave Theory and Techniques*, Scottsdale, AZ, pp. 2151-2159, 2008

[33] S. Capdevila, M. Jofre, J. Rodriguez, M. Guardiola, A. Papio, F. De Flaviis and L. Jofre, "UWB MST MEMS-based near-field imaging system", *IEEE 2008 Antennas and Propagation Society International Symposium*, San Diego, CA, pp. 1-4, 2008

[34] J. C. Rock, T. Hudson, B. Wolfson, D. Lawrence, B. Pillans, A. R. Brown and L. Coryell, "A MEMS-based, Ka-band, 16-element sub-array", *IEEE Aerospace conference*, Big Sky, MT, pp. 1-11, 2009

[35] S. Pranonsatit, A. S. Holmes, I. D. Robertson and S. Lucyszyn, "Single-pole eight-throw RF MEMS rotary switch", *Journal of Microelectromechanical Systems*, vol. 15, no. 6, pp. 1735-44, Dec. 2006

[36] S. Pranonsatit, A. S. Holmes and S. Lucyszyn, "Microwave modelling of RF MEMS rotary switches", *IET Microwaves, Antennas and Propagation*, 2011

[37] T. Thungren, E. L. Kollberg and K. S. Yngvesson, "Vivaldi antennas for single beam integrated receivers," in *European Microwave Conference*, Helsinki, Finland, pp. 361-366, 1982

[38] R. O. Lee and R.N. Simons, "Effect of curvature on tapered slot antennas", *Antennas and Propagation Society International Symposium*, Baltimore, MD, pp.188-191, 1996